© 2015. Published by The Company of Biologists Ltd | Development (2015) 142, 1492-1501 doi:10.1242/dev.110585

RESEARCH ARTICLE

The *vav* oncogene antagonises EGFR signalling and regulates adherens junction dynamics during *Drosophila* eye development

Maria-Dolores Martín-Bermudo[1], Pierre-Luc Bardet[2,*], Yohanns Bellaïche[2] and Marianne Malartre[1,3,4,‡]

ABSTRACT

Organ shaping and patterning depends on the coordinated regulation of multiple processes. The *Drosophila* compound eye provides an excellent model to study the coordination of cell fate and cell positioning during morphogenesis. Here, we find that loss of *vav* oncogene function during eye development is associated with a disorganised retina characterised by the presence of additional cells of all types. We demonstrate that these defects result from two distinct roles of Vav. First, and in contrast to its well-established role as a positive effector of the EGF receptor (EGFR), we show that readouts of the EGFR pathway are upregulated in *vav* mutant larval eye disc and pupal retina, indicating that Vav antagonises EGFR signalling during eye development. Accordingly, decreasing EGFR signalling in *vav* mutant eyes restores retinal organisation and rescues most *vav* mutant phenotypes. Second, using live imaging in the pupal retina, we observe that *vav* mutant cells do not form stable adherens junctions, causing various defects, such as recruitment of extra primary pigment cells. In agreement with this role in junction dynamics, we observe that these phenotypes can be exacerbated by lowering DE-Cadherin or Cindr levels. Taken together, our findings establish that Vav acts at multiple times during eye development to prevent excessive cell recruitment by limiting EGFR signalling and by regulating junction dynamics to ensure the correct patterning and morphogenesis of the *Drosophila* eye.

KEY WORDS: Vav, EGFR, Adherens junctions, Eye patterning, Morphogenesis

INTRODUCTION

Morphogenesis during animal development relies on cell fate specification together with correct organisation of cells and establishment of cell-cell junctions within epithelia. The coordination of these distinct processes is key to establishing normal cell function in a complex system. The *Drosophila* compound eye is ideally suited for dissection of the genetic and cellular requirements that govern pattern formation at molecular, cellular and tissue levels within an epithelium. The *Drosophila* adult eye is characterised by a very stereotyped organisation. One retina contains around 750 identical visual units called ommatidia, each ommatidium consisting of a precise number of cells that are specified during larval and pupal stages. During the third-instar larval stage, the eight photoreceptors (or R cells; neuronal) and the four lens-secreting epithelial cells (cone cells, CCs) differentiate in the eye imaginal disc, starting with the selection of an initial photoreceptor, the R8, from a pool of progenitor cells. R8 then recruits R2 and R5, which themselves recruit R3 and R4. After the second mitotic wave, R1, R6 and then R7 are added to the ommatidium, rapidly followed by selection of CCs. During pupal life, pigment cells differentiate from a pool of interommatidial pigment cells (IPCs). Two primary pigment cells are added first, enwrapping each cone cell cluster (lying on top of the eight photoreceptors) to form the core ommatidium. Excess interommatidial cells are eliminated by apoptosis, leaving the precise final cell number, and the remaining accessory cells ultimately differentiate as secondary and tertiary pigment cells along with sensory bristles, which completes formation of the hexagonal lattice that surrounds the core ommatidium (reviewed in Kumar, 2012). Different signalling pathways are used in combination to determine the different fates, among which Epidermal Growth Factor Receptor (EGFR) signalling is required for the differentiation of all cell types except R8. Expression of a dominant-negative EGFR completely prevents the formation of the retina (Freeman, 1996). Furthermore, the strength of EGFR signalling has to be tightly regulated by a balance between activators and inhibitors to allow the exact number of each cell type to be recruited to each ommatidium (Shilo, 2005; Yogev et al., 2008). Thus, ommatidium development is a model to understand how EGFR signalling can be modulated during development to allow correct cell fate specification.

Beside cell fate acquisition, cell-cell adhesion and intercalation are crucial for the different cells to be placed and held in their correct positions, representing another fundamental aspect of eye development and function. Several adhesion molecules such as N-Cadherin (Hayashi and Carthew, 2004), DE-Cadherin (Grzeschik and Knust, 2005) and proteins from the Nephrin and Neph1 families (Bao and Cagan, 2005) have been implicated in these cell-sorting processes to regulate accessory cell numbers, shapes and positions. Some regulators of cell-cell junctions in the retina have been identified, such as the CIN85 and CD2AP orthologue Cindr, an adaptor protein that assembles complexes, required to link cell surface adhesion molecules and the actin cytoskeleton to allow cell shape changes (Johnson et al., 2008). However, the mechanisms by which cell-cell junctions are stabilised while allowing cell movements remains elusive, and the identification of new regulators of junction dynamics will help our understanding of how tissue development is achieved.

One candidate that has been implicated in both mediating the EGFR signalling pathway and regulating cell adhesion is the guanine nucleotide exchange factor (GEF) Vav. The expression of Vav oncogenes in numerous human cancers (Lazer and Katzav, 2011) justifies a better understanding of their roles during tissue development and the characterisation of pathways with which they

[1]Centro Andaluz de Biología del Desarrollo CSIC-Univ. Pablo de Olavide, Sevilla 41013, Spain. [2]Institut Curie, CNRS UMR3215, INSERM U934, Paris Cedex 05 75248, France. [3]Université Paris-Sud, INSERM UMR-S757, Orsay 91405, France. [4]Centre de Génétique Moléculaire (UPR3404), CNRS, 1 avenue de la Terrasse, Gif-Sur-Yvette 91198, France.
*Present address: Inserm U1127/CNRS UMR7225, GH Pitié-Salpêtrière, Bâtiment ICM, Paris Cedex 13 75651, France.

‡Author for correspondence (marianne.malartre@u-psud.fr)

Received 26 March 2014; Accepted 2 March 2015

Development (2015) 142, 1492-1501 doi:10.1242/dev.110585

interact. Members of the Vav family are activated upon phosphorylation by cell surface receptors, and they can, in turn, activate the Rho GTPases by facilitating the exchange of a GDP for a GTP (Bustelo, 2000).

We previously demonstrated that the unique *Drosophila vav* gene is required for axon growth and guidance at different developmental stages in *Drosophila*, including guidance of photoreceptor axons from the larval eye disc into the optic lobe. We showed that *vav* is ubiquitously expressed in the eye disc, which is consistent with a possible function of Vav during eye development (Malartre et al., 2010).

Interestingly, mammalian Vav proteins are activated by tyrosine phosphorylation in response to EGFR induction, and their SH2 domains associate directly with the receptor both *in vitro* and *in vivo* (Bustelo et al., 1992; Margolis et al., 1992; Tamás et al., 2003). In *Drosophila*, Vav and the EGFR have been also shown to interact physically (Dekel et al., 2000; Sarkar et al., 2007) and genetically (Fernández-Espartero et al., 2013). These interactions and the ubiquitous expression of *vav* in the larval eye disc prompted us to examine whether Vav was involved in eye development and patterning and its relationship with EGFR signalling.

In this work, we show that Vav plays distinct roles during eye development to limit cell recruitment in the newly assembled ommatidium. Vav acts reiteratively in a GEF-dependent manner to recruit the correct number of photoreceptors, CCs and pigment cells. It does so, on the one hand, by downregulating the EGFR pathway, thus revealing a new interplay between Vav and the EGFR pathway. On the other hand, Vav regulates adhesion and the stability of cell-cell junctions to limit the number of primary pigment cells recruited.

RESULTS

vav mutant retinas display increased cell numbers at the apical surface

To determine whether the absence of *vav* caused a phenotype in the retina, we dissected *vav* pupal retinas once all cell recruitment and morphogenesis events are complete. We labelled them with the Discs large (Dlg) septate junctional marker, which allows the identification of all different cell types by shape and position (Fig. 1A). We found that *vav* retinas were disorganised and did not harbour the inter-weaving hexagonal lattice that characterises the wild-type ommatidia (Fig. 1A,B). A total of 18.75% of ommatidia (n=112 ommatidia from six retinas) were also misoriented along the equatorial-polar axis (Fig. 1C). In addition, many *vav* ommatidia contained extra cells of all types. To quantify this excess, we counted the number of cells forming the hexagonal lattice, which in wild-type is 18, including the four CCs, the two primary cells and the 12 accessory cells surrounding the ommatidia core (six secondary cells, three tertiary cells and three bristles) that are actually shared with neighbouring ommatidia (Fig. 1D). We found that *vav* ommatidia displayed an average of three extra cells per ommatidium (n=37 ommatidia, from four retinas). In addition to the excess in interommatidial cells (Fig. 1H), we observed that 32.1% (n=3620 ommatidia from 20 retinas) of *vav* ommatidia had extra CCs, ranging from five (85.5% of the cases, Fig. 1E) to eight CCs (Fig. 1G), and that 25.3% of *vav* ommatidia (n=1332 ommatidia from ten retinas) had extra primary

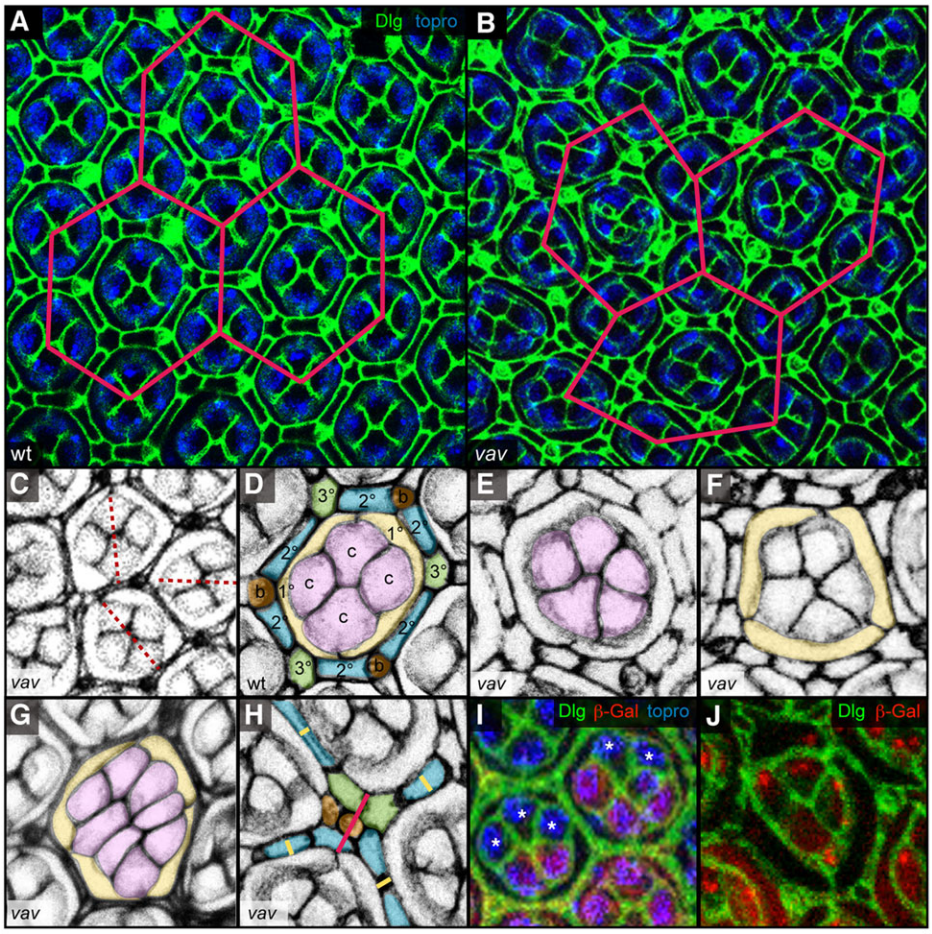

Fig. 1. Supernumerary cells at the apical surface of *vav* pupal retinas. Apical views of 50 h APF retinas stained with anti-Discs large (Dlg) antibody (green) and TOPRO (blue, nuclei). (A,B) To highlight the regular organisation of ommatidia in the retina, a hexagonal lattice is superimposed around a given ommatidium by joining the centre of the six surrounding ommatidia (in pink). (A) Wild-type (wt) retina showing the regularity in ommatidia organisation and cell number. (B) *vav* mutant retinas are disorganised, showing excessive cell numbers. (C-H) For better clarity, the Dlg signal in the image has been inverted so the staining appears in grey. (C) Dotted red lines indicate ommatidia orientations, highlighting misorientation of some ommatidia. (D) An example of wild-type ommatidium. The different cell types are pseudo-coloured for easier identification. CCs, pink; primary pigment cells (1°s), yellow; secondary (2°s) and tertiary (3°s) pigment cells, blue and green, respectively; bristles, brown. (E-G) *vav* ommatidia displaying five cone cells (E,F), three primary cells (F), and eight CCs and four primary cells (G). (H) Extra interommatidial cells in *vav* retina. In the interommatidial space, the yellow bars show the normal single cell layer, whereas the red bar indicates three cells instead of one. Colours are as in D. (I,J) *vav*FRT19A/*arm-lacZ*FRT19A; *eyflp*/+ retinas stained with anti-Dlg (green), anti-β-gal (red) and TOPRO (blue). *vav* clones are revealed by the absence of β-gal staining. (I) Ommatidia with extra CCs have at least one mutant CC (white asterisks). (J) Ommatidium with wild-type CCs and three primary cells.

Development (2015) 142, 1492-1501 doi:10.1242/dev.110585

cells (Fig. 1F,G). Similar results were obtained with other *vav* alleles (vav^{1}, vav^{2}, vav^{3} and vav^{11837}) and in clones (Fig. 1I for vav^{3}; supplementary material Fig. S3A for vav^{11837}), confirming that loss of Vav function causes a cell number increase.

vav mutant ommatidia possess extra photoreceptors

Having found that there are more cells than normal in the absence of Vav function at the apical retina, we investigated whether the number of photoreceptors lying underneath accessory cells was affected in *vav* retinas. To this end, we used an antibody against Elav, a neuronal marker that is expressed in all photoreceptors, and counted numbers of the R1-R7 photoreceptors that were present in the same focal plane and the number of the inner photoreceptor R8 located underneath R7. Seven photoreceptors per ommatidium were present on the same focal plane in wild-type retinas (n=91 ommatidia from four retinas, data not shown), as opposed to in *vav* mutant ommatidia, where 71.5% contained eight or more photoreceptors (n=233 ommatidia from four retinas, Fig. 2C). This was not due to a mis-localisation of R8s as another R cell per ommatidium was visible more basally in the retina (data not shown). This result shows that *vav* retinas are characterised by having a majority of ommatidia with at least one extra photoreceptor cell. This prompted us to analyse in more detail how R cells are specified during eye development in the absence of *vav*.

R7 photoreceptors are recruited in excess and prematurely in *vav* mutant ommatidia

To investigate whether the extra photoreceptors recruited in *vav* ommatidia belong to a specific R cell subtype or whether any subtype was recruited in excess, we used markers that are specific to individual R cell subtypes. In wild-type eye imaginal discs (supplementary material Fig. S1A), the presumptive R8 expresses *senseless* (*sens*) (Nolo et al., 2000). Occasional ommatidia with extra Sens-positive cells were found in *vav* eye discs (supplementary material Fig. S1B), although these cells were Elav-negative and excluded from ommatidia (supplementary material Fig. S1B″), suggesting that they failed to differentiate further as neurons. Hence, the extra Elav-positive cells found in 71.5% of *vav* ommatidia are unlikely to be of the R8 subtype.

In larval eye discs, the position of the extra R cells within each *vav* clusters suggested that they were R7s (supplementary material Fig. S1C-E). To confirm their identity, we used Prospero (Pros), a marker expressed in R7 (Kauffmann et al., 1996). Two or three Pros-expressing cells per ommatidium instead of one were often present in young *vav* ommatidia (Fig. 2A,B). These extra R7s were maintained throughout retina development, as pupal *vav* ommatidia with extra photoreceptors displayed two or more Pros-positive cells (Fig. 2C″). We then compared the timing of recruitment in wild-type and *vav* retinas. Spalt Major (Salm) and Pros expression in R7 starts in ommatidia rows seven and eight in wild-type larvae (Domingos et al., 2004; Kauffmann et al., 1996) (supplementary material Fig. S1C), and in rows five and six in *vav* discs (supplementary material Fig. S1D), suggesting that precocious recruitment of R7 takes place in the absence of *vav*. Taken together, our results show that Vav regulates the number and timing of R cell recruitment by limiting the excessive and premature acquisition of R7 fate.

Vav acts reiteratively during eye formation

The formation of an ommatidium is a stepwise process, starting with the selection of the R8. R cells recruit each other successively and send signals to select the four CCs. Pigment cells are recruited later by signalling emanating from the adjacent CCs (Kumar, 2012). Hence, there are at least two explanations for the presence of extra cells of all types in *vav* mutants: (1) the presence of extra accessory cells is a secondary consequence of recruiting extra R7s; or (2) Vav is acting reiteratively at each step of ommatidia assembly. To discriminate between these two hypotheses, we examined whether there was a correlation between the numbers of the different cell types observed in *vav* pupal retinas. Although some ommatidia had the correct number of CCs, primary cells (Fig. 3A) and photoreceptors (Fig. 3A′), others had more of the three cell types (Fig. 3A,A′). We also identified ommatidia with more CCs, although their R cell number was correct (Fig. 3B,B′,C,C′). This result shows that extra CCs can be produced in the absence of extra photoreceptors and therefore argues in favour of a reiterative role of Vav.

Similarly, no correlation was found between the number of CCs and primary cells because the following four types of ommatidia coexisted in *vav* retinas: those with excess CCs but the correct number of primary cells; those with the normal number of CCs but excess primary cells; those with the correct number of CCs and primary cells; and those with an excess of CCs and primary cells (Fig. 3D). Finally, among the ommatidia with five CCs (n=159 ommatidia from seven retinas), 54% had two primary cells, whereas 46% had three primary cells (Fig. 3E). Hence, an excess of primary cells is not a consequence of the presence of additional CCs. Taken together, our data suggest that Vav acts reiteratively during eye development to ensure that the correct number of each cell type is specified at each stage.

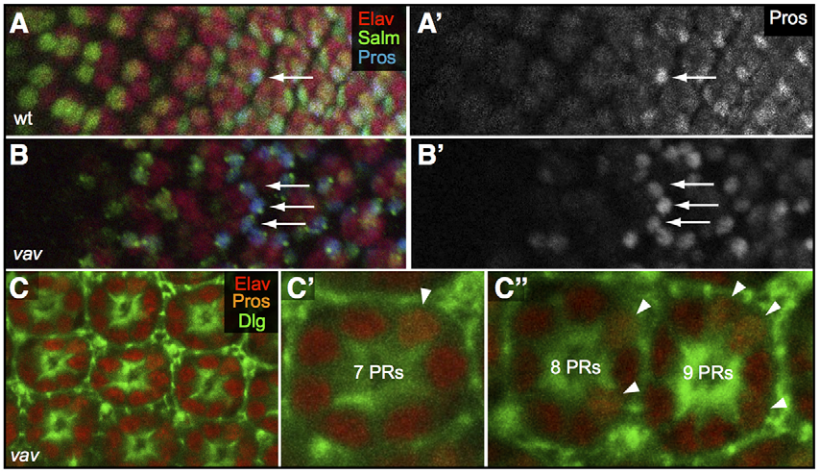

Fig. 2. Extra photoreceptors in *vav* eye disc and pupal retina. (A,B) Third-instar larval eye discs are oriented with anterior towards the left and stained with antibodies against Elav (red), Salm (green) and Pros (blue). Wild-type (wt) ommatidia possess a single R7 (arrow) identified by the expression of Pros (A), whereas *vav* ommatidia display multiple R7s that are recruited precociously (arrows) (B). (C) 48 h APF *vav* retina stained with antibodies against Elav (red), Pros (orange) and Dlg (green). Shown are projections of confocal sections underneath the apical surface of the pupal retina showing R1-R7 expressing Elav. R7s appear orange as they are positive for both Pros and Elav. Ommatidia with only seven R cells on the same plane possess only one R7 (arrowhead, C′), whereas ommatidia with extra R cells have multiple R7s (arrowheads, C″). The number of photoreceptor cells (PR) is indicated.

Development (2015) 142, 1492-1501 doi:10.1242/dev.110585

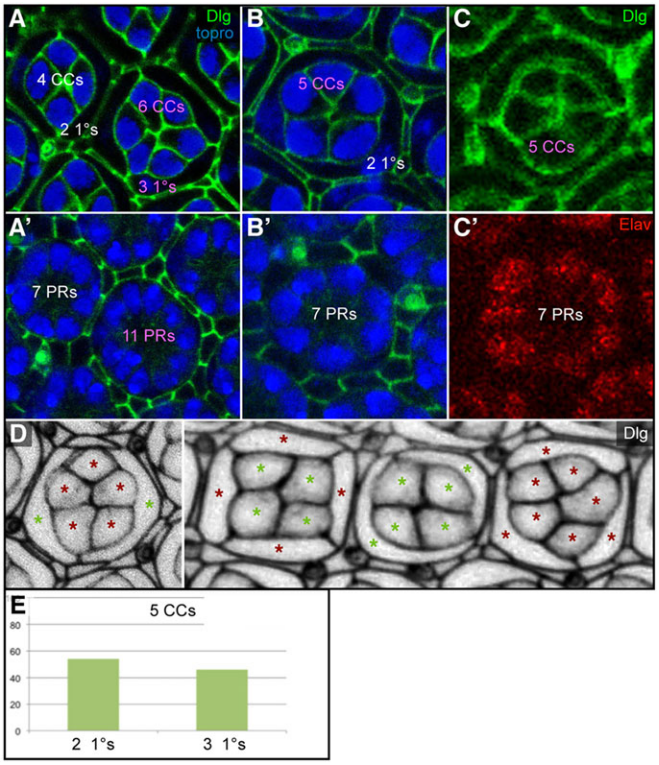

Fig. 3. *vav* phenotypes in the pupal retina are not correlated.
(A-D) 48 h APF *vav* retinas stained with anti-Dlg antibody (green in A-C; grey in D) and TOPRO (blue in A,B) or anti-Elav antibody (red in C′). Correct cell numbers (photoreceptors, PRs; cone cells, CCs; primary cells, 1°s) are indicated in white, incorrect numbers in pink. Apical surfaces (A-C) and the corresponding more basal sections to assess R cell numbers (A′-C′) are shown. (A,A′) Ommatidium with normal CC, primary (1°) and PR numbers, adjacent to an ommatidium with excess CC, primary and R cell numbers. (B-C) Ommatidia with extra CCs but correct photoreceptor numbers as identified by nuclei (B′) or Elav (C′) staining. (D) Asterisks indicate correct (green) and incorrect (red) numbers of CCs and primary cells. (E) Proportion of ommatidia with two or thee primary cells among ommatidia with five CCs, showing that there is no correlation between the two phenotypes.

Vav is a negative regulator of the EGFR signalling pathway

It is established that Vav is phosphorylated in response to EGFR stimulation (Margolis et al., 1992) and Vav loss-of-function is associated with decreased EGFR signalling in *Drosophila* cells (Hornstein et al., 2003). Therefore, Vav is proposed to act as a positive regulator of EGFR signalling. EGFR signalling is also used reiteratively during eye development to regulate cell recruitment (Freeman, 1996). However, and in contrast to what we found here for *vav* loss-of-function, decreasing EGFR signalling in the eye leads to a decrease in cell number, whereas increasing EGFR signalling causes over-recruitment of all cell types (Freeman, 1996) (Fig. 4A-C). In addition, *vav* eye discs display ommatidial rotation defects (supplementary material Fig. S2), consistent with the misoriented ommatidia observed in *vav* pupal retinas. Rotation defects and extra cells (including R7s) are also found in mutants for negative regulators of EGFR signalling, such as Sprouty and FasII (Casci et al., 1999; Mao and Freeman, 2009), as well as upon expression of dominant activators of EGFR pathway (Brunner et al., 1994; Strutt and Strutt, 2003). Thus, even though Vav has been so far shown to act positively downstream of the EGFR pathway, *vav* retina phenotypes are reminiscent of EGFR hyperactivity, suggesting that Vav has a new role as a negative regulator of EGFR signalling.

To investigate this hypothesis, we analysed the expression patterns of several readouts of the EGFR pathway in *vav* eye discs and retinas. First, we assessed the transcriptional activation of Kekkon, a specific EGFR target gene, which functions as a negative regulator of the pathway (Ghiglione et al., 2003). Higher levels of *kekkon-lacZ* were detected in *vav* clones (Fig. 4D,E), implying that EGFR signalling was hyper-activated in the absence of *vav*. We also used the phosphorylation of MAPK (known as Rolled in *Drosophila*) as another direct readout of EGFR signalling, which can be detected with the anti-diphosphoERK (diPERK) antibody. *vav* cells showed very high levels of diPERK compared with control tissue in mosaic pupal retinas (Fig. 4F,G). Interestingly, diPERK levels were increased in a cell-autonomous manner, indicating that EGFR signalling was upregulated autonomously in *vav* cells. Accordingly, *vav* mosaic ommatidia with CC excess all contained at least one *vav* mutant CC (n=62 ommatidia from 15 retinas) (Fig. 1I). Taken together, these results indicate that Vav acts autonomously as a negative regulator of EGFR signalling in the retina.

To further confirm this, we tested whether altering the levels of EGFR signalling had any effect on *vav* phenotypes. First, we inhibited the EGFR pathway in the eye by overexpressing Argos, a secreted protein that associates with Spitz, the EGFR ligand, therefore decreasing the quantity of ligand available. This resulted in an adult with a smaller eye with a rough aspect (Freeman, 1994) (Fig. 4H,J). This deleterious effect was largely rescued when removing *vav* (Fig. 4K), demonstrating that loss of *vav* function has an opposing effect to that of gain of *argos*. Second, we examined the consequences of halving the dose of Spitz in *vav* mutants. The *vav; spi*/+ retina organisation was largely rescued (compare Fig. 4M with 4N) confirming that Vav antagonises the EGFR signalling pathway during eye development.

Vav function in the retina relies on DH domain integrity

Most characterised Vav proteins' roles require their GEF function, although they have also been shown to act independently of GEF activity (Bustelo, 2000). To determine whether the new Vav role as an inhibitor of EGFR signalling depends on its GEF activity, and given that it is known that Rac proteins can be activated through the Vav GEF function (Bustelo, 2000; Couceiro et al., 2005), we first examined whether *Rac* and *vav* retinas displayed similar phenotypes. As opposed to the *vav* retina, excess CCs or primary cells were not observed in retina in which 90% of ommatidia were null for the three *Drosophila Rac* members, *Rac1*, *Rac2* and *Mtl* (supplementary material Fig. S3B). Occasional excess of interommatidial cells was observed, although the phenotype was milder than in *vav* retinas (supplementary material Fig. S3B). Given that the *vav* and *Rac* phenotypes in the retina are different, as opposed to the similar axon guidance phenotypes they display (Malartre et al., 2010), Rac proteins are unlikely to be the main Vav effectors for regulating cell recruitment in the eye, suggesting that Vav uses distinct effectors to regulate eye patterning and axon targeting.

We next generated new *vav* alleles using CRISPR/Cas9-mediated mutagenesis to create deletions in the DH domain that mediates GEF activity. Mice expressing enzymatically inactive but normally folded Vav1 protein ($Vav1^{AA}$) have been generated by introducing a point mutation that changed only two amino acids in the DH domain (Saveliev et al., 2009). Based on that work, and because these amino acids are conserved in *Drosophila*, we targeted the same region to create small deletions in the DH domain that are predicted to abolish GEF function. We obtained a mutant deleted for only one amino acid ($vav^{\Delta L}$) and a mutant deleted for three amino acids ($vav^{\Delta MQR}$, Fig. 5A,B). First, we confirmed that the GEF activity was

Development (2015) 142, 1492-1501 doi:10.1242/dev.110585

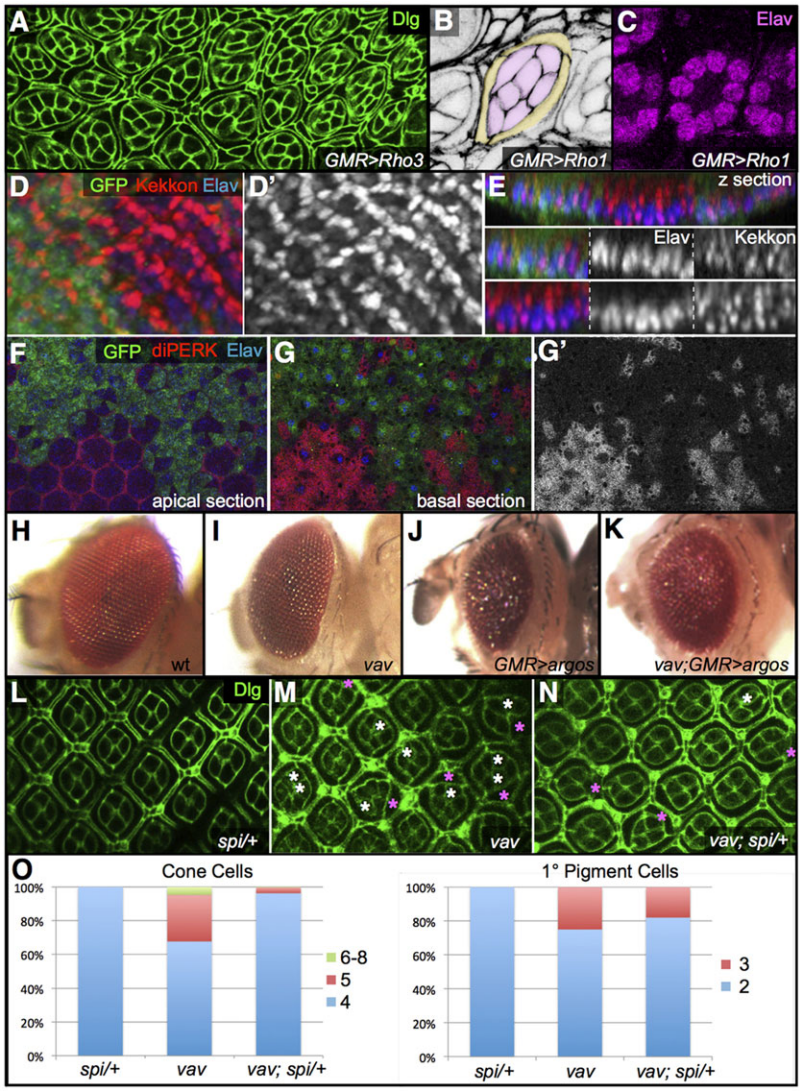

Fig. 4. Genetic interaction between *vav* and the *EGFR* signalling pathway. (A-C) 48 h APF retinas overexpressing *rhomboid1* (*GMR>Rho1*) or *rhomboid3* (*GMR>Rho3*) stained with antibodies against Dlg (green) and Elav (purple) showing that hyperactivation of EGFR pathway leads to an excess of all cell types in the retina. (B) An ommatidium with seven CCs (pink) and three primary cells (yellow). (C) A *z* projection of more basal sections from the same ommatidium showing nine photoreceptors. (D,E) Larval eye discs from *vav*FRT19A/*ubiGFPeyFlp*^{122}FRT19A; *kek-lacZ*/+ larvae stained with antibodies against GFP (green), β-gal (red) to detect Kekkon expression and Elav (blue). Orientation is with posterior towards the top. *vav* clones are identified by the lack of GFP staining. (D,D′) A portion of the disc showing control and *vav* cells. (E) A *z* section is shown at the top of the panel. Merged and separate channels of control (middle panel) and *vav* (bottom panel) regions of the same size. Kekkon expression is higher in *vav* tissue. (F,G) Retina from *vav*FRT19A/*ubiGFPeyFlp*^{122}FRT19A pupa stained with antibodies against GFP (green), diPERK (red) and Elav (blue) highlighting EGFR hyperactivation in the absence of Vav. (H-K) Adult *Drosophila* eyes. (I) Eyes from *vav* adult escapers. (J) Argos over-expression in the eye driven by GMR-Gal4 gives a rough and smaller eye. (K) This effect is largely suppressed in *vav* mutants. (L-N) 50 h APF retinas stained with anti-Dlg antibody (green). (L) Decreasing a dose of the EGFR ligand Spitz (*spi*/+) does not affect retina patterning nor cell number. (M) *vav* retina showing extra CCs (white asterisks) and extra primary cells (pink asterisks). (N) In *vav; spi*/+ retina, the CC excess phenotype is almost completely rescued, although extra primary cells are still present. (O) Quantification of the CC and primary cell (1°) numbers, illustrating that decreasing a copy of *spi* in the *vav* mutant leads to an almost complete rescue in CC number (97% of ommatidia), although the proportion of ommatidia with extra primary cells is not altered substantially.

compromised in these new DH point mutation alleles, as they all exhibited phenotypes similar to those of *vav* and *Rac* nulls during axonal targeting (Malartre et al., 2010; data not shown). Interestingly, these mutants also exhibited phenotypes similar to those associated with the *vav*-null alleles in the retina, with lower penetrance only for the single amino acid deletion (Fig. 5C-F). The vav$^{\Delta MQR}$ deletion was sufficient to recapitulate the strength of *vav*-null phenotypes indicating that Vav function in the eye requires its GEF activity. Similarly, we generated mutations in the C-terminal domain of Vav that deleted either both the SH2 and SH3 domains or only the SH3 domain (Fig. 5A). Phenotypic analysis showed that the loss of the SH2 and SH3 domains fully impaired Vav function in the retina, whereas the loss of the SH3 domain alone had no effect (Fig. 5E,F). Taken together, our analyses indicate that both Vav GEF activity and the binding of Vav to the EGFR are necessary to inhibit EGFR signalling. This suggests that both recruitment to the EGFR and downstream signalling activity mediated by activation of GTPases are necessary to perform this unexpected inhibitory function of Vav.

vav mutant retinas display mis-patterning phenotypes that account for junction or adhesion defects

To investigate whether all *vav* eye phenotypes were rescued by decreasing EGFR levels, we compared the numbers of the different cell types in *vav* and *vav*; *spi*/+ retinas. We found that the extra CCs phenotype was almost completely rescued as only 4.3% of *vav; spi*/+ ommatidia displayed extra CCs (n=2253 ommatidia from eight retinas), compared with the 32.1% found in *vav* retinas (Fig. 4O). In sharp contrast, the extent of the rescue was different for the primary cells as the proportion of ommatidia with extra primary cells was only slightly lower in *vav; spi*/+ retina (18.1%, n=1114 ommatidia from four retinas) as compared with *vav* (25.3%, see Fig. 4O). This result supports our earlier conclusion that the recruitment of extra primary cells in *vav* retinas is not a consequence of extra CCs. Furthermore, it points to the possibility that some extra primary cells observed in *vav* retinas are due to a Vav function that is independent of its effect on EGFR signalling.

In response to EGFR signalling, the CCs produce the Delta ligand to induce the specification of primary cells (Nagaraj and Banerjee, 2007). However, a mosaic *vav* ommatidium with all wild-type CCs can still have an excess of primary cells (Fig. 1J). This indicates that the excess of primary cells in *vav* retinas is not only due to an increase in Delta-Notch signalling from the CC to the primary precursor.

Extra primary cells can also be caused by defective cell movements (Johnson et al., 2008; Johnson and Cagan, 2009). To determine whether cell-cell junction stability or adhesion could be affected in *vav* retinas, we assessed the ommatidial mis-patterning score (OMS), a

Development (2015) 142, 1492-1501 doi:10.1242/dev.110585

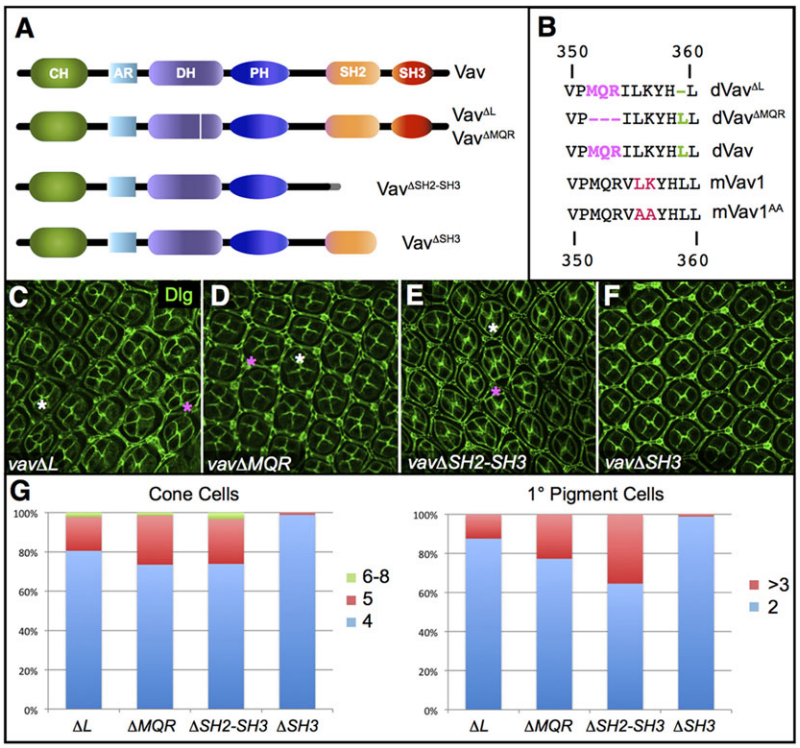

Fig. 5. Mutation in the Vav DH domain and SH2 deletion abrogates its function in the retina. (A) Schematic representation of the different mutants obtained from the Crispr/Cas9-mediated mutagenesis. CH, calponin homology; AR, acidic rich region; DH, dbl homology; PH, pleckstrin homology; SH2, Src homology 2; SH3, Src homology 3. The grey bar in $vav^{\Delta SH2\text{-}SH3}$ construct represents the 30 amino acids introduced by the frame shift before the stop codon. (B) Amino acid sequence in the DH domain is given for wild-type *Drosophila* Vav (dVav) and deletion mutants, together with the corresponding sequence for mice Vav1 (mVav1) and $Vav1^{AA}$. (C-F) Apical views of 50 h APF retinas stained with anti-Dlg antibody showing that, like in *vav*-null mutants, excess CCs and primary cells are found in $vav^{\Delta L}$, $vav^{\Delta MQR}$ and $vav^{\Delta SH2\text{-}SH3}$ mutants, but not in $vav^{\Delta SH3}$ mutants. Extra CCs and extra primary cells are indicated by white and pink asterisks, respectively. (G) Quantification of the CC and primary (1°) numbers from the different genotypes. For CCs, n=314 ommatidia from one retina ($vav^{\Delta L}$), 1641 ommatidia from seven retinas ($vav^{\Delta MQR}$), 687 ommatidia from three retinas ($vav^{\Delta SH2\text{-}SH3}$) and 912 ommatidia from two retinas ($vav^{\Delta SH3}$). For primary cells, n=233 ommatidia from one retina ($vav^{\Delta L}$), 1355 ommatidia from seven retinas ($vav^{\Delta MQR}$), 660 ommatidia from three retinas ($vav^{\Delta SH2\text{-}SH3}$) and 912 ommatidia from two retinas ($vav^{\Delta SH3}$).

means of scoring a broad range of specific traits (Johnson and Cagan, 2009). We found that *vav* retina scored nine errors per ommatidium on average (n=43 from six retinas). Among these errors, the following can result from junction or adhesion defects: incorrect orientation of CC junctions (supplementary material Fig. S4B), energetically unstable CCs arrangement (supplementary material Fig. S4C), non-equivalent primary cell sizes (supplementary material Fig. S4D), and non-equivalent primary-primary cell junction sizes, with extreme cases where one of the two junctions was completely lost (supplementary material Fig. S4F). Taken together, this suggests that Vav could be involved in cell rearrangement, by forming or stabilising CC and primary-primary cell junctions or by controlling cell movements during pupal eye morphogenesis.

vav mutant cells are excessively dynamic causing extra primary cell recruitment and patterning delay

To further analyse the hypothesis that Vav is involved in junction stability or remodelling, we compared the dynamics of adherens junction rearrangements by time-lapse microscopy in wild-type and *vav* pupae from the time of primary cell recruitment (between 16 h and 19 h APF). Live imaging was performed by visualising the expression of a knock-in GFP in the DE-cadherin (*shotgun*) gene (*shg:GFP*, Huang et al., 2009) in wild-type retina and in *vav* clones, as identified by the lack of ubi-GFP. To analyse whether specification of supernumerary primary cells was associated with abnormal cell movements, we tracked cell junction dynamics during primary cell formation. In wild-type retina, the two primary cell candidates adopt an elongated shape, get in contact to form a collar around the CC cluster at ~19 h APF and establish stable adherens junctions (Fig. 6A; supplementary material Movie 1) (Larson et al., 2008; Johnson and Cagan, 2009). We identified three phenotypes that support the hypothesis that Vav plays a role in adherens junction dynamics. First, we observed excessive switching of primary cell precursors with surrounding cells, leading to excessive remodelling of adherens junctions without defects in the final number of primary cells (supplementary material Fig. S5B, Movie 2). These abnormal movements sometimes occurred for hours and in several cells around a single ommatidium (supplementary material Fig. S5C, Movie 3). Importantly, this resulted in a patterning delay (supplementary material Fig. S5A) without causing recruitment of extra primary cells. Similar abnormal movements have been observed in retina defective for *cindr* activity (Johnson et al., 2008).

Second, we found that the defects in junction dynamics correlated with the recruitment of extra primary cells. Indeed, we observed cases (n=6 movies out of nine) where two proto-primary cells got in contact several times to enwrap the CC cluster, before failing to establish a stable junction and maintain their niches, allowing a third cell to intercalate and adopt the typical primary cell shape (Fig. 6B; supplementary material Movie 4).

Finally, we observed cases where the two primary cells either failed to establish a stable junction after several attempts in making contact or had already established junctions but failed to maintain one of them. This led to an open primary cell phenotype where the CCs enter in direct contact with the IPCs instead of being enwrapped (Fig. 6C; supplementary material Movie 5). Taken together, our live imaging analyses show that excessive cell movements take place in the absence of *vav*, and imply that Vav stabilises cell-cell junctions and prevents abnormal movements. This results in cells that are more dynamic, which can be associated with the recruitment of extra primary cells.

vav interacts genetically with *shg* and *cindr*

To further support the role of Vav in junction dynamics and adhesion, we tested whether decreasing adherens junction function in *vav* retinas amplified the supernumerary primary cell phenotype. Reducing adhesion by using a hypomorphic allele of *shotgun* ($shg^{P34\text{-}1}$), the *Drosophila* E-cadherin, did not affect retina patterning (Fig. 7A). Strikingly, using the same $shg^{P34\text{-}1}$ allele strongly enhanced the *vav* phenotype – from 25% of ommatidia with extra primary cells to

Development (2015) 142, 1492-1501 doi:10.1242/dev.110585

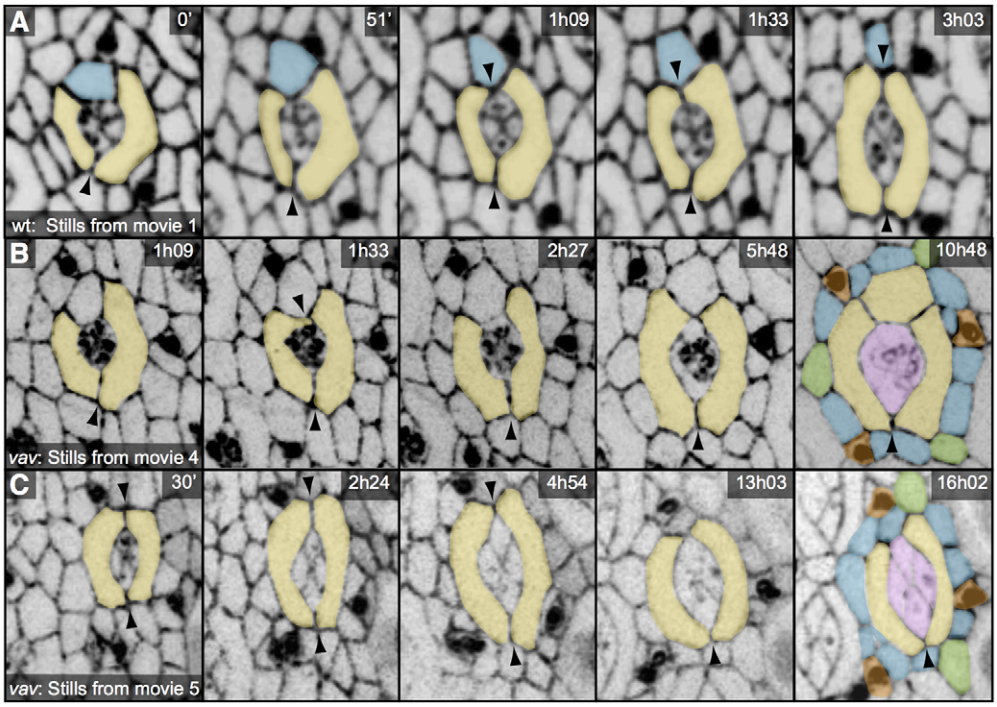

Fig. 6. Unstable primary-primary cell junctions are associated with various phenotypes in *vav* retina. Live imaging from wild-type (wt) pupal retina (A) and *vav* clones (B,C). The time at which the different pictures were taken is indicated. (A) Wild-type ommatidium from a *DE-cadherin:*GFP pupa, showing that once two primary cells (yellow) enter in contact (arrowheads), a stable junction is established. (B,C) Pupae of the following genotype were selected: *vav*FRT19A/*ubiGFPeyFlp*^{122}FRT19A; *DE-cadherin:GFP*/+. *vav* ommatidia from clonal regions are presented. (B) Over several hours, two primary cells (yellow) enter in contact and are separated successively. As they fail to establish a stable junction, a third cell intercalates, leading to the recruitment of three primary cells. Note that extra primary cells are unlikely to be due to IPC crowding, as extra primary cells in *vav* ommatidia followed by live imaging were not associated with an increase of IPC number at the time of primary cell recruitment, as compared with *vav* ommatidia with two primary cells (mean of 14.3 and 14.4 cells, respectively; *n*=14 ommatidia with two and 14 with three final primary cells). (C) A junction between two primary cells that had been maintained for several hours is finally disrupted. Hence, the CC cluster (pink) enters in contact with the interommatidial cells (blue), leading to the open primary cell phenotype. Tertiary pigment cells are in green and bristles in orange.

61.5% in *vav; shg*$^{P34\text{-}1}$ (Fig. 7C,G, *n*=1289 ommatidia from six retinas). Interestingly, and in agreement with our proposal that extra CCs are mainly due to defects in EFGR signalling, the percentage of ommatidia with extra CCs was similar in *vav* (32.2%) and *vav; shg*$^{P34\text{-}1}$ (32.9%, *n*=1342 ommatidia from six retinas, Fig. 7G).

Reducing the activity of Cindr, an adaptor protein that interacts with Cadherin and multiple components of the actin cytoskeleton, also affects cell movements during retina patterning (Johnson et al., 2008). Interestingly, *cindr* phenotypes are also enhanced in a heterozygous *shg* background, and live imaging movies of pupal

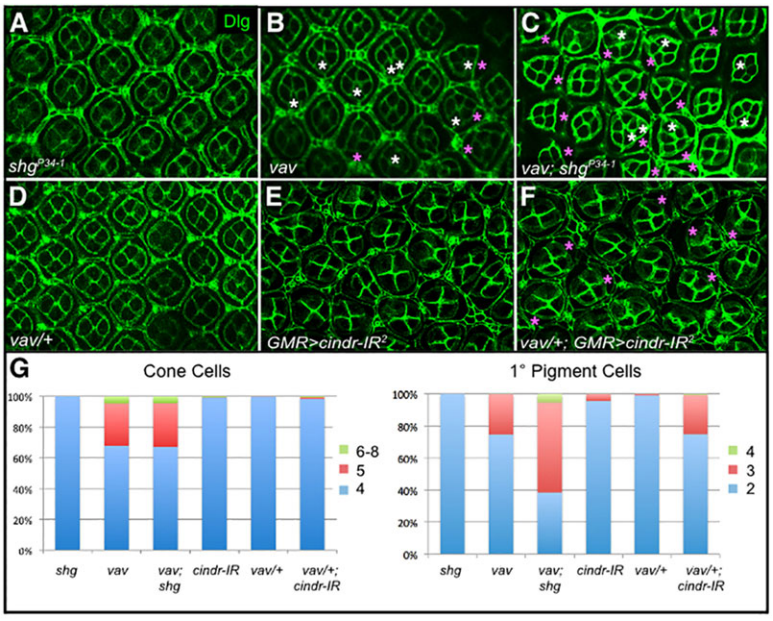

Fig. 7. *vav* interacts genetically with *DE-cadherin* and *cindr*. Apical views of 50 h APF retinas stained with anti-Dlg antibody. (A) Retina patterning and cell number are not affected by *shg*$^{P34\text{-}1}$, a hypomorphic allele for *DE-cadherin*. (B) *vav* retina showing extra CCs (white asterisks) and extra primary cells (pink asterisks). (C) In *vav; shg*$^{P34\text{-}1}$ mutants, the extra primary cells phenotype is increased whereas CC number is not. (D) Retina patterning and cell number are not affected in *vav*/+ retina. (E) *GMR>cindr-IR*^{2} retina display a series of patterning defects, including disorganisation of the retina, misplaced pigment cells and bristles, excess of IPCs, ommatidia misrotation, CC cluster arrangement, and a mild excess of primary cells. (F) In *vav*/+; *GMR>cindr-IR*^{2} retinas, the extra primary cells phenotype is increased. (G) Quantification illustrates that decreasing adhesion in the *vav* mutant or decreasing *vav* levels in the presence of *cindr* RNAi increases the primary cell (1°) but not CC excess [0.8% of ommatidia in *GMR>cindr-IR*^{2} (*n*=1154 ommatidia from eight retinas) and 1.6% in *vav*/+; *GMR>cindr-IR*^{2} (*n*=1437 ommatidia from seven retinas)].

Development (2015) 142, 1492-1501 doi:10.1242/dev.110585

eyes with reduced *cindr* activity showed that there was junction instability and primary cell replacement in these retinas. We therefore tested whether *vav* and *cindr* interacted genetically. To address this question, we expressed a *cindr* RNA interference (RNAi) line in wild-type eyes (*GMR>cindr-IR*^{2}) and in a *vav* heterozygous background (*vav/+; GMR>cindr-IR*^{2}). Decreasing *cindr* function leads to a series of patterning defects, including a mild excess of primary cells (Fig. 7E) (Johnson et al., 2008). Whereas in *vav* heterozygous retinas, cell numbers were close to those in wild-type (98.9% and 99.9% of ommatidia with normal primary and CC numbers, respectively; *n*=1099 ommatidia from four retinas), halving the *vav* dose in *cindr-IR*^{2} retinas enhanced the *cindr-IR*^{2} phenotypes (Fig. 7F). As shown in Fig. 7G, this was particularly striking for the number of ommatidia with three primary cells [4.4% of ommatidia in *GMR>cindr-IR*^{2} (*n*=1154 ommatidia from eight retinas) versus 25.1% in *vav/+*; *GMR>cindr-IR*^{2} (*n*=1198 ommatidia from seven retinas)]. These results indicate that *vav* and *cindr* interact genetically, in particular for the recruitment of primary cells, and are in agreement with a model where Vav, like Cindr, participates in a signalling pathway linking the cell-surface junctions with components of the actin cytoskeleton.

DISCUSSION

In this study, we provide evidence for distinct roles of the *vav* gene in regulating cell shaping and patterning of the *Drosophila* eye. On the one hand, Vav acts reiteratively to limit cell recruitment by counteracting EGFR signalling, and, on the other hand, it regulates adhesion and junction dynamics to limit excessive cell recruitment.

The EGFR signalling pathway is antagonised by Vav

The EGFR is a well-characterised signal transducer that has been highly conserved during evolution (Shilo, 2003). EGFR activity is subject to modulation by multiple regulators to ensure that the appropriate level of signalling is provided to specific cells (Bogdan and Klämbt, 2001). The increasing number of positive and negative regulators identified highlights the fundamental role of this well-conserved cascade during animal development. The *Drosophila* eye has provided a very good model to identify new EGFR regulators because subtle changes in the multiple cycles of EGFR activation lead to changes in cell numbers that can be easily identified due to the specific compound structure of this organ (Shilo, 2005; Kumar, 2012). Vav is activated by tyrosine phosphorylation in response to cell surface receptors and, in particular, its interaction with the EGFR through its SH2-binding domain has been extensively demonstrated (Bustelo et al., 1992; Margolis et al., 1992; Tamás et al., 2003; Dekel et al., 2000; Sarkar et al., 2007). Our work now provides compelling evidence supporting an additional role for Vav as an antagonist of EGFR signalling activity. Importantly, we demonstrate that this unexpected activity requires both functional DH and SH2 domains. Two non-exclusive models could account for Vav negative regulation of EGFR signalling in a GEF-dependent manner. First, Vav could downregulate the EGFR pathway by reducing the number of receptors available at the cell surface. In support of this model, it has been shown that mammalian Vav GEFs are required for endocytosis of both ephrin, during axon guidance (Cowan et al., 2005), and B cell antigen receptor, which is in many ways similar to receptor tyrosine kinase internalisation (Malhotra et al., 2009). Second, Vav could stimulate the transcription of negative regulators of the EGFR pathway, such as Kekkon. Accordingly, Vav members were demonstrated to regulate gene transcription through the activation of Rho GTPases, although the mechanism by which this occurs is still unknown (Vigorito et al., 2003; Citterio et al., 2012). Taken together, our findings showing that Vav can antagonise the EGFR pathway unveil the complexity of the relationships between these two proteins in different cell types. They highlight the necessity of further investigation on the basis of these additional regulations during animal development as well as in the context of cancer given that both Vav and the EGFR are overexpressed in numerous human cancers (Lazer and Katzav, 2011; Nicholson et al., 2001).

Regulation of junction dynamics and adhesion

The regulation of cell-cell junction dynamics and adhesion is fundamental for epithelial morphogenesis and reshaping, and various members of the Rho GTPases and their GEF regulators have been implicated in these processes during *Drosophila* embryonic (reviewed in Takeichi, 2014) and eye (Warner and Longmore, 2009a,b; Yashiro et al., 2014) development. Recently, with the development of live imaging tools, the use of the *Drosophila* eye has proven to be an excellent system to study the role of adhesion and junction dynamics *in vivo* (Larson et al., 2008). In particular, the recruitment of primary cells depends on both the integration of combinatorial signalling pathways (Nagaraj and Banerjee, 2007) and the regulation of cell-cell adhesion (Bao, 2014). Once the first two primary cell candidates are selected, they have to form stable junctions that enwrap the CCs and isolate them to prevent additional primary cell recruitment from the IPC pool. Accordingly, Cindr acts on E-Cadherin and the actin cytoskeleton to maintain adherens junctions, thus limiting excessive movements leading to extra primary cell recruitment (Johnson et al., 2008). Our live imaging experiments showed that junctions between primary cells were unstable in the absence of Vav, causing various patterning defects. Because *vav* genetically interacts with *E-Cadherin* and *cindr*, and given that the ortholog of *cindr*, known as CIN85 or CD2AP, directly associates with Vav in human B cells (Niiro et al., 2012), we can envision that Vav might act with Cindr to modulate cell junction stability in the retina (both proteins being part of a complex and providing a link between junction proteins such as Cadherins and the actin cytoskeleton). Taken together, our data reveals a new Vav function in the regulation of adherens junction dynamics in the *Drosophila* eye.

In summary, Vav, which is located at the crossroads of distinct signalling pathways, is playing different roles during eye development, from recruitment of photoreceptors and accessory cells to photoreceptor axon targeting, but is also involved in cell dynamics and junction remodelling to ensure the well-ordered generation of appropriate numbers of the different cell types forming the perfectly structured *Drosophila* eye.

MATERIALS AND METHODS

Drosophila genetics

All crosses were conducted at 25°C. The following fly strains were provided by Bloomington *Drosophila* Stock Center: the *Canton S* strain as the wild-type reference, *salm-lacZ*, UAS-*argos*, *spi*^{1}, *GMR*-Gal4, *shotgun*$^{P34\text{-}1}$. Other fly strains used were: *vav*^{1}, *vav*^{2}, *vav*^{3}*FRT19A* (Malartre et al., 2010), *vav*^{11837}*FRT19A* (Kyoto Stock Center), yw, *ubiGFPeyFlp*^{122}FRT19A (Kevin Legent, IJM, Paris), FRT19A*arm-lacZ;* eyFLP/TM6b (a gift from Fernando Casares, CABD, Seville, Spain), UAS-*Rhomboid1* and UAS-*Rhomboid3* (a gift from Matthew Freeman, University of Oxford, Oxford, UK), *kekkon-lacZ* (Christian Ghiglione, IBV, Nice, France), *trio*^{1}*FRT80B* (a gift from Barry Dickson, IMP, Vienna, Austria), *yweyFLP gl-lacZ; 3Lclw+FRT80Mtl*$^{\Delta}$ and *rac1*^{j11}*rac2*$^{\Delta}$*FRT80Mtl*$^{\Delta}$ (a gift from Takashi Suzuki, TIT, Yokohama, Japan), *E-cadherin:GFP* (a gift from Yang Hong, University of Pittsburgh, Pittsburgh, PA, USA) and *cindr-IR*^{2} line (a gift from Ruth Johnson, Wesleyan University, Middletown, CT, USA). Unless otherwise specified, *vav*^{2} and *vav*^{3} were both used in experiments conducted on whole mutant retinas and *vav*^{3}*FRT19A* was used in clonal analyses.

Development (2015) 142, 1492-1501 doi:10.1242/dev.110585

Generation of *vav* alleles using Crispr/Cas9

New *vav* alleles were generated by CRISPR- and Cas9-mediated non-homologous end joining. Two pairs of guide RNA (gRNA) target sites were used: 5′-GTACTTGAGAATGCGCTGCATGG-3′ and 5′-TCTCAAGTA-CCATCTGCTGCTGG-3′ surrounding the LK amino acids necessary for the GEF activity (Saveliev et al., 2009) and the 5′-GTCAGTTGTCCGAG-TTCAATTGG-3′ and 5′-GTGGCGATCACCTCCTTGTAGGG-3′ located respectively at the 5′ and 3′ of the Vav SH2 domain (amino acids 622 to 730). gRNAs were cloned in the pCFD3-dU6:3gRNA plasmid (Addgene). Pairs of gRNAs (250 ng/µl each) were injected (BestGene) in embryos (600 for each pair) laid by Vasa-Cas9 females (Gratz et al., 2014). 278 F0 and 735 F1 crosses were established and progenies were screened by a T7 endonuclease assay (Zhang et al., 2014), by PCR or by lethality to identify deletions in the DH or SH2 domains. Deletions were further mapped by sequencing. $vav^{\Delta SH2\text{-}SH3}$ is a 41-nucleotide deletion leading to a frame shift in which 30 different amino acids are followed by a stop codon. $vav^{\Delta SH3}$ is a 10-nucleotide deletion leading to a frame shift that removes the six last amino acids of the SH2 domain and introduces one amino acid followed by a stop codon, thus removing the entire SH3 domain.

Mosaic analysis

vav mutant clones were obtained using the FLP-FRT technique (Xu and Rubin, 1993). Recombination was induced by eyeless FLP activity. Mutant clones were marked by the absence of anti-GFP or anti-β-galactosidase antibody staining. Genotypes used for clonal analysis in larvae were: vav^{3}FRT19A/*arm-lacZ*FRT19A*; eyflp*/+, vav^{11837}FRT19A/*arm-lacZ*FRT19A*; eyflp*/+, vav^{3}FRT19A/yw, *ubiGFPeyFlp*^{122}FRT19A*; kek-lacZ*/+. *Rac1*^{J11} *rac2*$^{\Delta}$ *mtl*$^{\Delta}$ triple null clones were generated from the following pupae: *yweyFLP gl-lacZ; 3Lclw+FRT80Mtl*$^{\Delta}$*/rac1*^{j11}*rac2*$^{\Delta}$*FRT80Mtl*$^{\Delta}$. 3Lcl is a minute mutation leading to 90% of eye cells being mutant, as confirmed in the adult eye by the lack of w+.

Immunohistochemistry

Immunostaining was performed according to standard procedure and as described previously (Walther and Pichaud, 2007). For pupal dissection, white prepupae were collected (0 h after puparium formation, APF) and staged at 25°C. The following primary antibodies were used: mouse anti-Dlg (1:50), rat anti-Elav (1:500), mouse anti-Pros (1:10), mouse anti-Cut (1:100) (Developmental Studies Hybridoma Bank); rabbit anti-Salm (1:500, kind gift from Fernando Casares), guinea pig anti-Sens (1:1000, a kind gift from Hugo Bellen, BCM, Houston, TX, USA), mouse anti-diPERK (1:100, Sigma, dissection into PBS containing 1 µM okadaic acid prior to fixation), rabbit anti-GFP (1:1000, Molecular Probes), and mouse anti-β-galactosidase (1:5000, Promega) antibodies. To label nuclei, retinas were incubated with the DNA dye TO-PRO-3 (1:1000, Molecular Probes). The secondary antibodies labelled with Alexa Fluor 488, Alexa Fluor 568 (Molecular probes) or Cy5 (Jackson ImmunoResearch) were used at 1:200. Samples were mounted in Vectashield (Vector Laboratories), and images captured with a Leica TCS-SP2 or a Nikon eclipse TE 2000-U confocal microscope and the EZ-C1 3.30 software. Confocal image stacks were processed with ImageJ software (1.46r).

Time-lapse experiments

Pupae were mounted as described in Bardet et al., 2013. Images were acquired with a Ropper spinning-disk confocal mounted on an Eclipse Ti microscope (Nikon) using the Metamorph software. We imaged eight *vav* mutant mosaic retinas between 15-35 h APF. In the clonal region, and after elimination of ommatidia for which focus was lost or that moved out of frame during the course of the movie, morphogenesis was reconstituted and analysed for 36 ommatidia.

Image treatments

Raw fluorescence images were processed to increase the signal to noise ratio (Kervrann and Boulanger, 2006). After a maximum projection of the image stacks, the different parts of the eye filmed separately were stitched and registered using the Fiji plug-in 'Stitching' (Preibisch et al., 2009) and 'StackReg', respectively.

Acknowledgements

We thank Kevin Legent, Fernando Casares, Matthew Freeman, Christian Ghiglione, Yang Hong, Hugo Bellen, Barry Dickson, Takashi Suzuki, Ruth Johnson, the Kyoto Stock Center and the Bloomington Drosophila Stock Center for providing reagents; Isabelle Gaugué and Sana Dieudonné for their help during the Crispr screen; Ross Cagan, Dario Coen, Colin Sharpe and Anne-Marie Pret for helpful comments and discussions; and the Curie imaging facility (PICT-IBiSA@BDD, UMR3215/U934) for help and advice.

Competing interests

The authors declare no competing or financial interests.

Author contributions

M.M. performed the experiments and analysed the data. M.M. and P.-L.B. designed and performed the live imaging. M.M. and Y.B. conceived the experiments and wrote the paper. P.-L.B. and M.-D.M.B. edited the manuscript.

Funding

This work was supported by Spanish Ministerio de Ciencia y Tecnología [BFU2013-48988-C2-1-P]; Junta de Andalucía [CVI-280 and PO6-CVI1592]; European Research Council (ERC) Starting (CePoDro); ERC Advanced (TiMorp); and the Programme Labellisé Fondation ARC [SL220130607097].

Supplementary material

Supplementary material available online at
http://dev.biologists.org/lookup/suppl/doi:10.1242/dev.110585/-/DC1

References

Bao, S. (2014). Notch controls cell adhesion in the Drosophila eye. *PLoS Genet.* **10**, e1004087.

Bao, S. and Cagan, R. (2005). Preferential adhesion mediated by Hibris and Roughest regulates morphogenesis and patterning in the Drosophila eye. *Dev. Cell* **8**, 925-935.

Bardet, P.-L., Guirao, B., Paoletti, C., Serman, F., Léopold, V., Bosveld, F., Goya, Y., Mirouse, V., Graner, F. and Bellaïche, Y. (2013). PTEN controls junction lengthening and stability during cell rearrangement in epithelial tissue. *Dev. Cell* **25**, 534-546.

Bogdan, S. and Klämbt, C. (2001). Epidermal growth factor receptor signaling. *Curr. Biol.* **11**, R292-R295.

Brunner, D., Oellers, N., Szabad, J., Biggs, W. H., III, Zipursky, S. L. and Hafen, E. (1994). A gain-of-function mutation in Drosophila MAP kinase activates multiple receptor tyrosine kinase signaling pathways. *Cell* **76**, 875-888.

Bustelo, X. R. (2000). Regulatory and signaling properties of the Vav family. *Mol. Cell. Biol.* **20**, 1461-1477.

Bustelo, X. R., Ledbetter, J. A. and Barbacid, M. (1992). Product of vav proto-oncogene defines a new class of tyrosine protein kinase substrates. *Nature* **356**, 68-71.

Casci, T., Vinós, J. and Freeman, M. (1999). Sprouty, an intracellular inhibitor of Ras signaling. *Cell* **96**, 655-665.

Citterio, C., Menacho-Márquez, M., García-Escudero, R., Larive, R. M., Barreiro, O., Sánchez-Madrid, F., Paramio, J. M. and Bustelo, X. R. (2012). The rho exchange factors vav2 and vav3 control a lung metastasis-specific transcriptional program in breast cancer cells. *Sci. Signal.* **5**, ra71.

Couceiro, J. R., Martín-Bermudo, M. D. Bustelo, X. R. (2005). Phylogenetic conservation of the regulatory and functional properties of the Vav oncoprotein family. *Exp. Cell Res.* **308**, 364-380.

Cowan, C. W., Shao, Y. R., Sahin, M., Shamah, S. M., Lin, M. Z., Greer, P. L., Gao, S., Griffith, E. C., Brugge, J. S. and Greenberg, M. E. (2005). Vav family GEFs link activated Ephs to endocytosis and axon guidance. *Neuron* **46**, 205-217.

Dekel, I., Russek, N., Jones, T., Mortin, M. A. and Katzav, S. (2000). Identification of the Drosophila melanogaster homologue of the mammalian signal transducer protein, Vav. *FEBS Lett.* **472**, 99-104.

Domingos, P. M., Brown, S., Barrio, R., Ratnakumar, K., Frankfort, B. J., Mardon, G., Steller, H. and Mollereau, B. (2004). Regulation of R7 and R8 differentiation by the spalt genes. *Dev. Biol.* **273**, 121-133.

Fernández-Espartero, C. H., Ramel, D., Farago, M., Malartre, M., Luque, C. M., Limanovich, S., Katzav, S., Emery, G. and Martín-Bermudo, M. D. (2013). GTP exchange factor Vav regulates guided cell migration by coupling guidance receptor signalling to local Rac activation. *J. Cell Sci.* **126**, 2285-2293.

Freeman, M. (1994). Misexpression of the Drosophila argos gene, a secreted regulator of cell determination. *Development* **120**, 2297-2304.

Freeman, M. (1996). Reiterative use of the EGF receptor triggers differentiation of all cell types in the Drosophila eye. *Cell* **87**, 651-660.

Ghiglione, C., Amundadottir, L., Andresdottir, M., Bilder, D., Diamonti, J. A., Noselli, S., Perrimon, N. and Carraway, K. L., III (2003). Mechanism of inhibition of the Drosophila and mammalian EGF receptors by the transmembrane protein Kekkon 1. *Development* **130**, 4483-4493.

Gratz, S. J., Ukken, F. P., Rubinstein, C. D., Thiede, G., Donohue, L. K., Cummings, A. M. and O'Connor-Giles, K. M. (2014). Highly specific and efficient CRISPR/Cas9-catalyzed homology-directed repair in Drosophila. *Genetics* **196**, 961-971.
Grzeschik, N. A. and Knust, E. (2005). IrreC/rst-mediated cell sorting during Drosophila pupal eye development depends on proper localisation of DE-cadherin. *Development* **132**, 2035-2045.
Hayashi, T. and Carthew, R. W. (2004). Surface mechanics mediate pattern formation in the developing retina. *Nature* **431**, 647-652.
Hornstein, I., Mortin, M. A. and Katzav, S. (2003). DroVav, the Drosophila melanogaster homologue of the mammalian Vav proteins, serves as a signal transducer protein in the Rac and DER pathways. *Oncogene* **22**, 6774-6784.
Huang, J., Zhou, W., Dong, W., Watson, A. M. and Hong, Y. (2009). Directed, efficient, and versatile modifications of the Drosophila genome by genomic engineering. *Proc. Natl. Acad. Sci. USA* **106**, 8284-8289.
Johnson, R. I. and Cagan, R. L. (2009). A quantitative method to analyze Drosophila pupal eye patterning. *PLoS ONE* **4**, e7008.
Johnson, R. I., Seppa, M. J. and Cagan, R. L. (2008). The Drosophila CD2AP/CIN85 orthologue Cindr regulates junctions and cytoskeleton dynamics during tissue patterning. *J. Cell Biol.* **180**, 1191-1204.
Kauffmann, R. C., Li, S., Gallagher, P. A., Zhang, J. and Carthew, R. W. (1996). Ras1 signaling and transcriptional competence in the R7 cell of Drosophila. *Genes Dev.* **10**, 2167-2178.
Kervrann, C. and Boulanger, J. (2006). Optimal spatial adaptation for patch-based image denoising. *IEEE Trans. Image Process* **15**, 2866-2878.
Kumar, J. P. (2012). Building an ommatidium one cell at a time. *Dev. Dyn.* **241**, 136-149.
Larson, D. E., Liberman, Z. and Cagan, R. L. (2008). Cellular behavior in the developing Drosophila pupal retina. *Mech. Dev.* **125**, 223-232.
Lazer, G. and Katzav, S. (2011). Guanine nucleotide exchange factors for RhoGTPases: good therapeutic targets for cancer therapy? *Cell. Signal.* **23**, 969-979.
Malartre, M., Ayaz, D., Amador, F. F. and Martin-Bermudo, M. D. (2010). The guanine exchange factor vav controls Axon growth and guidance during Drosophila development. *J. Neurosci.* **30**, 2257-2267.
Malhotra, S., Kovats, S., Zhang, W. and Coggeshall, K. M. (2009). B cell antigen receptor endocytosis and antigen presentation to T cells require Vav and dynamin. *J. Biol. Chem.* **284**, 24088-24097.
Mao, Y. and Freeman, M. (2009). Fasciclin 2, the Drosophila orthologue of neural cell-adhesion molecule, inhibits EGF receptor signalling. *Development* **136**, 473-481.
Margolis, B., Hu, P., Katzav, S., Li, W., Oliver, J. M., Ullrich, A., Weiss, A. and Schlessinger, J. (1992). Tyrosine phosphorylation of vav proto-oncogene product containing SH2 domain and transcription factor motifs. *Nature* **356**, 71-74.
Nagaraj, R. and Banerjee, U. (2007). Combinatorial signaling in the specification of primary pigment cells in the Drosophila eye. *Development* **134**, 825-831.
Nicholson, R. I., Gee, J. M. and Harper, M. E. (2001). EGFR and cancer prognosis. *Eur. J. Cancer* **37** Suppl. 4, 9-15.
Niiro, H., Jabbarzadeh-Tabrizi, S., Kikushige, Y., Shima, T., Noda, K., Ota, S.-i., Tsuzuki, H., Inoue, Y., Arinobu, Y., Iwasaki, H. et al. (2012). CIN85 is required for Cbl-mediated regulation of antigen receptor signaling in human B cells. *Blood* **119**, 2263-2273.
Nolo, R., Abbott, L. A. and Bellen, H. J. (2000). Senseless, a Zn finger transcription factor, is necessary and sufficient for sensory organ development in Drosophila. *Cell* **102**, 349-362.
Preibisch, S., Saalfeld, S. and Tomancak, P. (2009). Globally optimal stitching of tiled 3D microscopic image acquisitions. *Bioinformatics* **25**, 1463-1465.
Sarkar, A., Parikh, N., Hearn, S. A., Fuller, M. T., Tazuke, S. I. and Schulz, C. (2007). Antagonistic roles of Rac and Rho in organizing the germ cell microenvironment. *Curr. Biol.* **17**, 1253-1258.
Saveliev, A., Vanes, L., Ksionda, O., Rapley, J., Smerdon, S. J., Rittinger, K. and Tybulewicz, V. L. J. (2009). Function of the nucleotide exchange activity of vav1 in T cell development and activation. *Sci. Signal.* **2**, ra83.
Shilo, B.-Z. (2003). Signaling by the Drosophila epidermal growth factor receptor pathway during development. *Exp. Cell Res.* **284**, 140-149.
Shilo, B.-Z. (2005). Regulating the dynamics of EGF receptor signaling in space and time. *Development* **132**, 4017-4027.
Strutt, H. and Strutt, D. (2003). EGF signaling and ommatidial rotation in the Drosophila eye. *Curr. Biol.* **13**, 1451-1457.
Takeichi, M. (2014). Dynamic contacts: rearranging adherens junctions to drive epithelial remodelling. *Nat. Rev. Mol. Cell Biol.* **15**, 397-410.
Tamás, P., Solti, Z., Bauer, P., Illés, A., Sipeki, S., Bauer, A., Faragó, A., Downward, J. and Buday, L. (2003). Mechanism of epidermal growth factor regulation of Vav2, a guanine nucleotide exchange factor for Rac. *J. Biol. Chem.* **278**, 5163-5171.
Vigorito, E., Billadeu, D. D., Savoy, D., McAdam, S., Doody, G., Fort, P. and Turner, M. (2003). RhoG regulates gene expression and the actin cytoskeleton in lymphocytes. *Oncogene* **22**, 330-342.
Walther, R. F. and Pichaud, F. (2007). Immunofluorescent staining and imaging of the pupal and adult Drosophila visual system. *Nat. Protoc.* **1**, 2635-2642.
Warner, S. J. and Longmore, G. D. (2009a). Distinct functions for Rho1 in maintaining adherens junctions and apical tension in remodeling epithelia. *J. Cell Biol.* **185**, 1111-1125.
Warner, S. J. and Longmore, G. D. (2009b). Cdc42 antagonizes Rho1 activity at adherens junctions to limit epithelial cell apical tension. *J. Cell Biol.* **187**, 119-133.
Xu, T. and Rubin, G. M. (1993). Analysis of genetic mosaics in developing and adult Drosophila tissues. *Development* **117**, 1223-1237.
Yashiro, H., Loza, A. J., Skeath, J. B. and Longmore, G. D. (2014). Rho1 regulates adherens junction remodeling by promoting recycling endosome formation through activation of myosin II. *Mol. Biol. Cell* **25**, 2956-2969.
Yogev, S., Schejter, E. D. and Shilo, B.-Z. (2008). Drosophila EGFR signalling is modulated by differential compartmentalization of Rhomboid intramembrane proteases. *EMBO J.* **27**, 1219-1230.
Zhang, X., Ferreira, I. R. S. and Schnorrer, F. (2014). A simple TALEN-based protocol for efficient genome-editing in Drosophila. *Methods* **69**, 32-37.

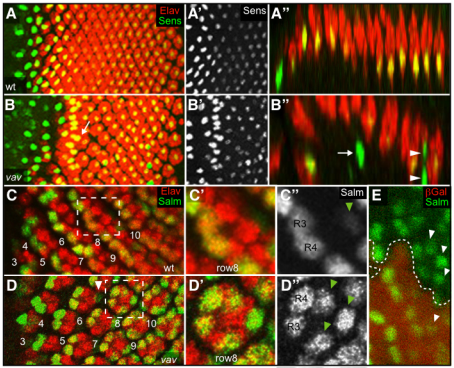

Figure S1. Extra R7 cells are recruited precociously to forming ommatidia in *vav* mutant larval eye discs.

Third-instar larval eye discs are oriented with anterior towards the left. **(A-B)** Co-staining with antibodies against Elav (red) and Sens (R8, green) reveals that ectopic R8s are recruited in *vav* discs (arrow). Z projection images. **(A)** Wild-type. **(B)** *Vav* disc. **(A″-B″)** Re-slicing the stack of images revealed that extra R8s actually fail to differentiate further as neurons as seen by the lack of Elav staining, and fail to recruit more R cells as there are isolated. Extra R8s are located underneath (arrow) or in between (arrowheads) ommatidia. **(C-D)** Discs from salm-lacZ larvae stained with anti-Elav antibody (red) to mark neurons and anti-β-gal antibody (green) to mark R3/R4. Rows of ommatidial differentiation are indicated. **(C′, C″, D′, D″)** Enlargements of the regions outlined in C and D. **(C′, D′)** Merged channels. **(C″, D″)** Salm staining (green channel). **(C)** In *salm-lacZ*/+ larvae, Salm expression is restricted to only two cells, the R3 and R4 until row 7. Salm expression starts to be detected in three cells in row 8, with a weak expression in the putative R7 (arrowhead). **(D)** In *vav; salm-lacZ*/+ larvae, Salm expression is restricted to R3/R4 until row 5 only. White arrowhead indicates a putative R7 in row 6. In row 8, Salm is strongly expressed in five cells, with three putative R7s, also supported by the cell position in the cluster (arrowheads). **(E)** *vav*FRT19A/*arm-lacZ*FRT19A; *eyflp*/+ larval eye disc stained with β-gal (red) to identify vav mutant tissue (no β-gal) and Salm to visualized R3, R4 and R7. The limit of the clone is highlighted by the dotted line. Five Salm-positive cells are present in vav mutant ommatidia, whereas wild-type ommatidia display only three positive cells on the same row, showing extra R cell recruitment in the vav mutant cells. Putative R7s are indicated by arrowheads.

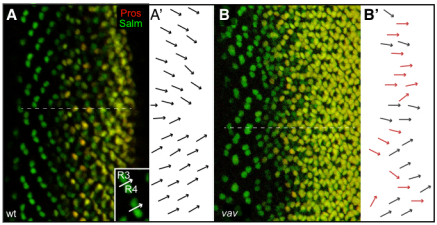

Figure S2. Ommatidia rotation defects in *vav* mutant larval eye discs.

(A-B) Third-instar larval eye discs are oriented with anterior towards the left. At the time R3 and R4 are specified, the developing ommatidial cluster rotate 90° in the dorsal and ventral halves of the eye on each side of the dorsoventral midline, also called the equator (represented by a dotted line). Anti-Pros antibody (red) and anti-β-gal antibody (green) to mark R3/R4 were used. **(A)** *Salm-lacZ* larva. Ommatidia close to the morphogenetic furrow (to the left) are perpendicular to the equator. Around row 6, ommatidia have rotated 45°, and in the posterior part of the disc, the 90° rotation is almost complete. Tracing an arrow between R3 and R4 gives the orientation of a single ommatidium (inset). **(A')** Arrows were traced on top of the picture in A, and the picture was removed to highlight the orientation of ommatidia in the first rows of differentiation. Correct orientations are indicated by black arrows **(B)**. *Vav; salm-lacZ* larva. In addition to the extra cells phenotype, many ommatidia display rotation defects. **(B')** Mis-rotated ommatidia are indicated by red arrows.

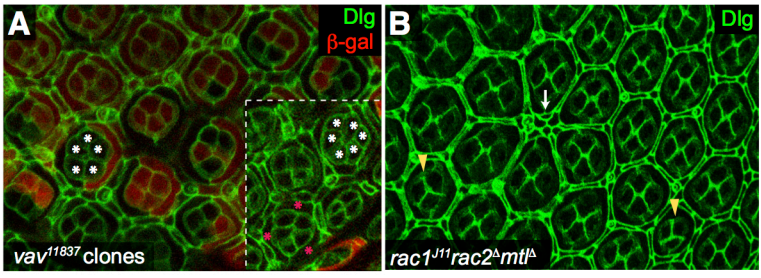

Figure S3. Triple *rac* cells do not display the same phenotypes as *vav* in the eye.

(A) *Vav11837*FRT19A/*arm-lacZ*FRT19A; *eyflp*/+ pupae were dissected and retinae stained with anti-Dlg antibody (green) and anti-β-gal (red) antibody. *Vav11837* allele displays the same phenotypes as the *vav1, vav2* and *vav3* alleles. *Vav* mutant clones are revealed by the absence of β-gal staining. The extra CC phenotype is highlighted by white stars and the extra 1° phenotype by pink stars. The image in the inset comes from a different retina. **(B)** Retina almost entirely mutant for *rac1, rac2,* and *mtl* were generated. As opposed to *vav* mutant, no ommatidia with extra CCs nor 1°s are found. A few ommatidia even displayed the opposite phenotype with less CCs (yellow arrowheads, 5.7%, n= 450 from 3 retinae) . Only extra interommatidial cells (arrow) are detected, although the phenotype was less frequent and milder than in *vav* retina.

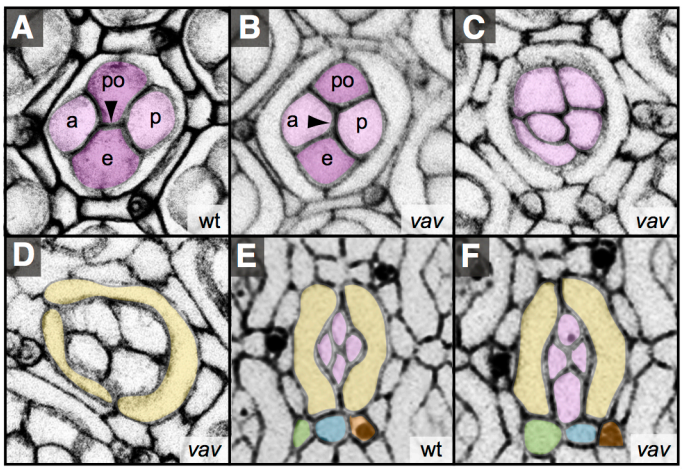

Figure S4. *Vav* mutant phenotypes related to putative junctional or adhesion defects at the retinal apical surface.

Apical views of 48 h APF retinae stained with anti-Dlg antibody to visualize septate junctions **(A-D)** or anti-Armadillo antibody to visualize adherens junctions **(E-F)**. The different cell types are pseudo-coloured for easier identification: CCs in pink, 1°s in yellow, 2°s and 3°s in blue and green respectively, bristles in brown. **(A)** In wild-type, polar (po) and equatorial (e) CCs are in contact at the centre of the cluster, whereas anterior (a) and posterior (p) CCs are separated. In *vav* tissue, defects in the CC cluster include orientation of CC junctions (64% of ommatidia) **(B)** and CCs not arranged in an energetically stable manner that is normally used to maximise adhesion between cells (37% of the ommatidia) **(C)**. **(D)** 1°s of different sizes (23% of ommatidia). **(E)** In wild-type, the two 1°s are forming a collar around the CC cluster. **(F)** In *vav* ommatidia, defects in junctional integrity leads to an opening between the two 1°s, so the CC cluster enters in contact with the IPC (Open 1° phenotype, 7% of ommatidia).

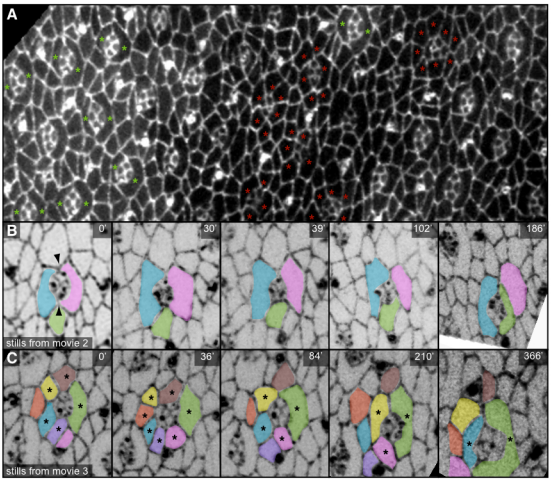

Figure S5. Unstable 1°:1° junctions cause cells to be highly dynamics and delay cell recruitment in *vav* mutants.

(A) Pupa of the following genotype was selected: *vavFRT*19A/*ubiGFPeyFlp122*FRT19A; *DE-cadherin:GFP*/+. Adherens junctions are marked by the DE-cadherin: GFP. *Vav* cells are identified by the lack of ubi-GFP. At the time wild-type ommatidia have recruited the two 1°s that enwrap the CC cluster (green stars), *vav* ommatidia are still surrounded by three to eight 1°-candidates (red stars). **(B-C)** Live imaging of *vav* ommatidia. Cells that are finally selected as 1°s are pseudo-coloured in blue and green for better clarity. **(B)** *vav* cells from a clonal region, showing that an established contact between two 1°s can be lost (at 30′). The 1°-like cell in pink that has adopted the typical elongated shape of 1°s is finally displaced by the 3°-like cell in green that changes its shape when it reaches the position to become a 1°. **(C)** *vav* cells are highly dynamics and compete to become 1°s. Cells in direct contact with the CC cluster are identified by black stars, showing that cells that are separated from the CC cluster can re-enter in contact with it (5 cells in contact at 0′ and 7 cells in contact at 36′). The yellow 1°-like elongated cell (at 210′) is displaced by the blue cell (366′) although the latest had totally lost contact with the CC cluster.

Supplementary Material Movie 1. Dynamics of wild type ommatidia assembly shown in Fig. 5A.

Live imaging of wild-type development on *DE-cadherin:GFP* pupa. Eyes were imaged at 2 min intervals. Primary pigment cell formation shows that once two 1°-like establish a contact, a junction is formed and maintained.

Supplementary Material Movie 2. Dynamics of the *vav* phenotype shown in Fig. S5B.

Live imaging of primary pigment cell formation defect in a *vav* mutant clonal region from *vav*FRT19A/*ubiGFPeyFlp*^{122}FRT19A; *DE-cadherin:GFP*/+ pupae. At the beginning of the movie, 1° selection seems to have occurred as two 1°-like cells with their typical elongated shape surround the CC cluster. However, an invading cell from the IPC is able to completely displace a previously established 1°-like cell from the CC cluster it was contacting, disrupting the 1°:1° junction, so the first pre-1° is moved to the interommatidial space. Eyes were imaged at 3 min intervals.

Supplementary Material Movie 3. Dynamics of the *vav* phenotype shown in Fig. S5C.

Cell competition for the 1° niche in a *vav mutant clonal region*. Cells surrounding the CC cluster are excessively motile and more than two cells compete during hours to become 1°s. Some of them initially contact the CCs, are displaced by adjacent cells exhibiting 1°-like behaviour, and then re-enter in contact with the CCs. One of these cells is eventually selected as the 1°. Eyes were imaged at 3 min intervals.

Supplementary Material Movie 4. Dynamics of the three 1°s phenotype shown in Fig. 5B.

Live imaging of *vav* mutant development in a clonal region. Three cells compete for the 1° niche. Two 1°-like establish and loose contact several times but a third cell finally stays in the middle leading to the recruitment of three 1°s around the CC cluster. Eyes were imaged at 3 min intervals.

Supplementary Material Movie 5. Dynamics of the open 1° phenotype shown in Fig. 5C.

Live imaging of *vav* mutant development in a clonal region. Two 1°s had established junctions but one of the junctions is lost after several hours. As a consequence, the CC cluster enters in contact with the interommatidial cells. Eyes were imaged at 3 min intervals.

Supplementary Material Movie 1

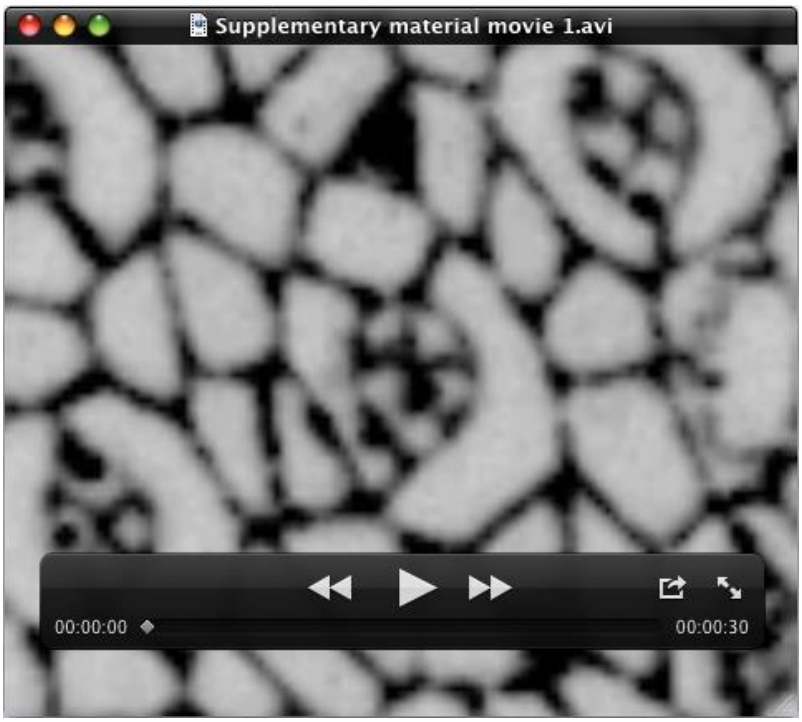

Supplementary Material Movie 2

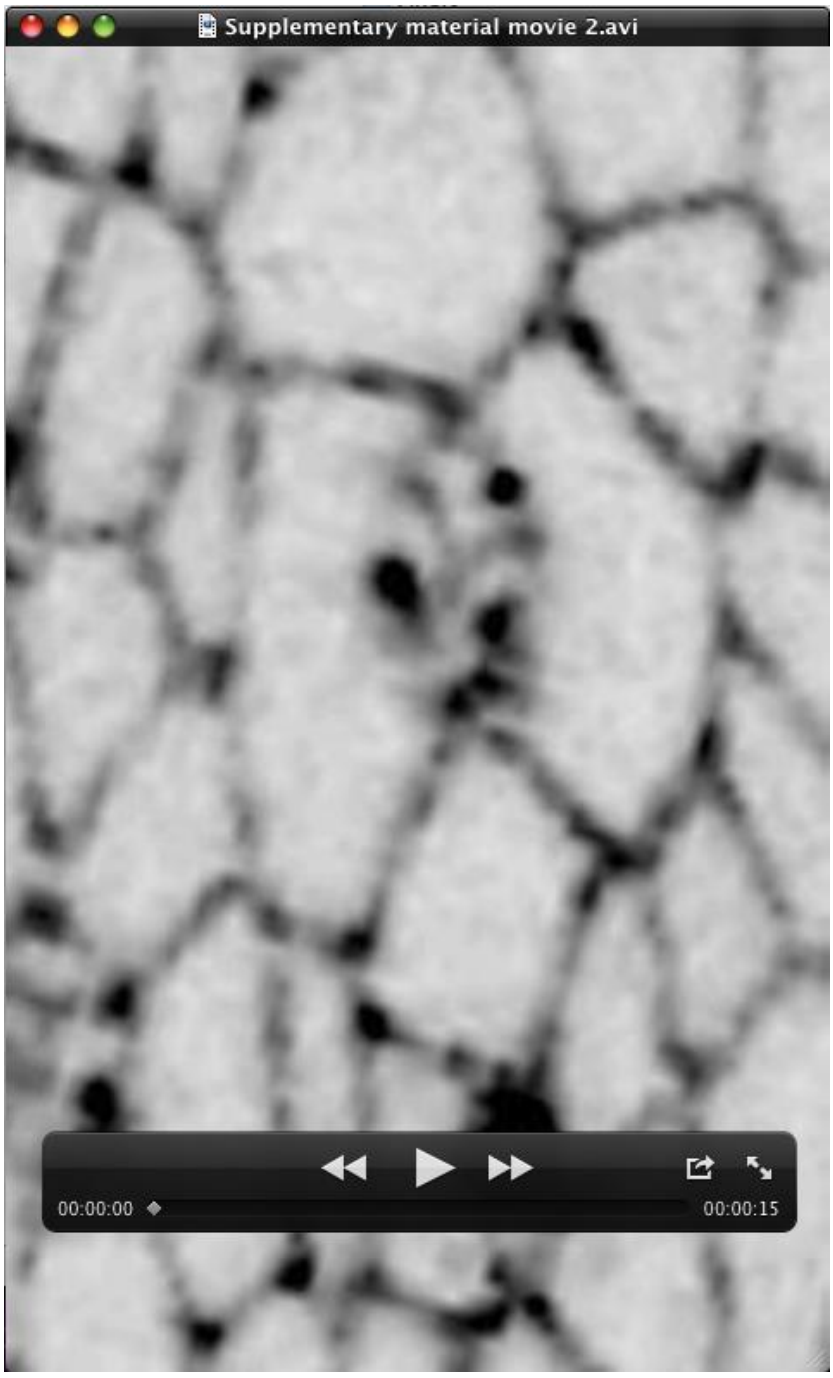

Supplementary Material Movie 3

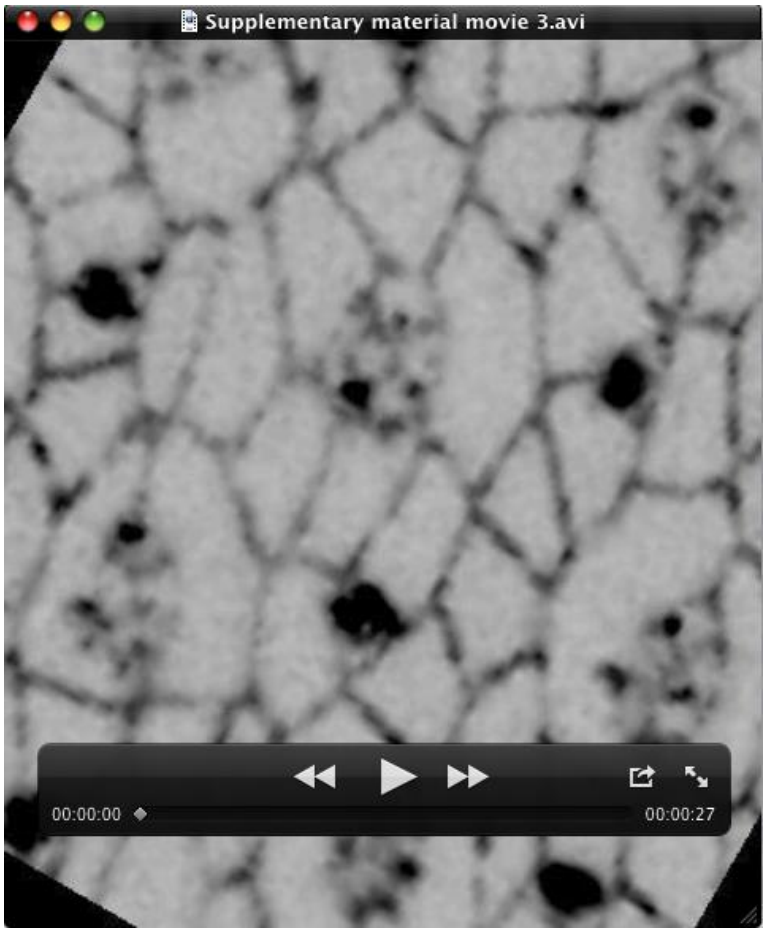

Supplementary Material Movie 4

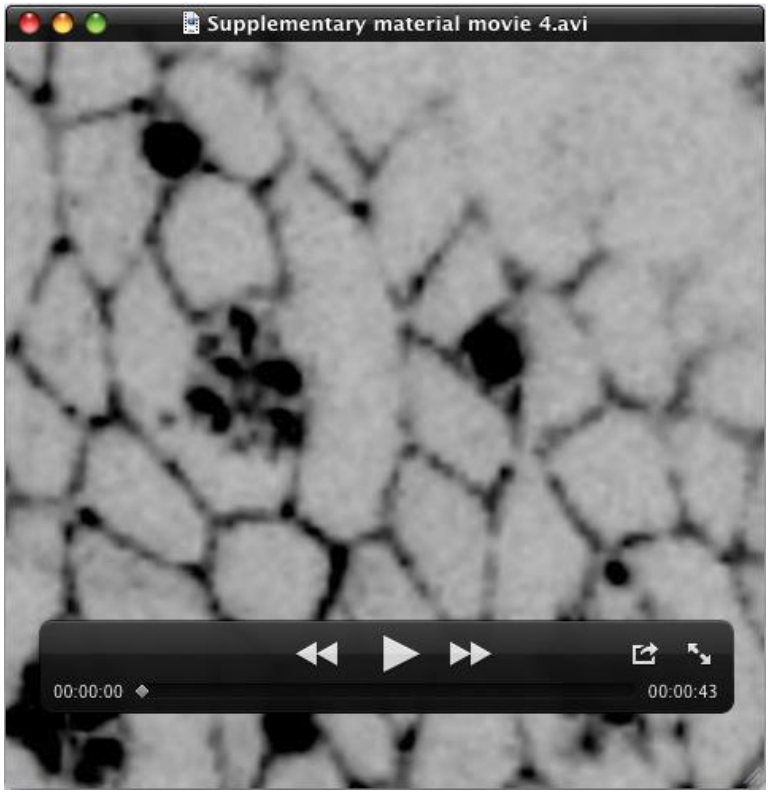

Supplementary Material Movie 5